Paper 44

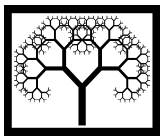

Proceedings of the Ninth International Conference
on Engineering Computational Technology,
P. Iványi and B.H.V. Topping, (Editors),
Civil-Comp Press, Stirlingshire, Scotland.

Multiple Crack Propagation in Friction Stir Welded Aluminium Joints

R. Citarella[1], P. Carlone[1], R. Sepe[2] and M. Lepore[1]
[1]Department of Industrial Engineering
University of Salerno, Italy
[2]Department of Chemical, Materials and Production Engineering
University of Naples Federico II, Italy

Abstract

This paper is concerned with the simulation of crack propagation in friction stir welded butt joints, in order to assess the influence of process induced microstructural alterations and residual stresses on the fatigue behaviour of the assembly. The approach employed is based on the coupled use of the finite element method and the dual boundary element method in order to take advantage of the main capabilities of the two methods. The distribution of the process induced residual stresses has been mapped by means of the *contour method*. Then, the computed residual stresses field has been superimposed, in a dual boundary element environment, to the stress field as a result of a remote fatigue traction load and the crack growth is simulated. A two-parameter crack growth law, based on the evaluation of two thresholds, for the material being analysed, is used for the crack propagation rate assessment. The stress intensity factors are evaluated using the J-integral technique. Computational results have been compared with experimental data, provided from constant amplitude crack propagation tests on welded samples, showing the subdivision of the overall fatigue life in the two periods of crack initiation and crack propagation.

Keywords: friction stir welding, residual stress, microstructure, finite element method, dual boundary element method.

1 Introduction

Medium to high strength aluminium alloys are currently considered of great interest in the transport industries. In particular, the precipitation hardenable AA2024 (Al-Cu) alloy is gaining considerable attention for aeronautical applications. In this context, remarkable research effort is focused on the application of the Friction Stir Welding (FSW) process, as a suitable alternative to fusion welding processes. Indeed, the poor dendritic microstructure and the high porosity in the weld zone,

induced using conventional techniques, strongly reduce the mechanical behaviour of the assembly. Furthermore, the reduction of production costs and weight and the increase of strength and damage tolerance with respect to riveted lap joints make FSW a very attractive process to aerospace industry. However, a deeper understanding of static strength as well as of fatigue behaviour of FSWed assemblies is highly desired for a wider implementation of the technique in safety-critical components.

FSW is a solid-state welding process, developed and patented by The Welding Institute (TWI) of Cambridge in 1991. During the process a non-consumable rotating tool, constituted by a shoulder and a pin, is plunged between the adjoining edges of the parts to be welded and moved along the desired weld line. The combined rotation and translation of the tool locally increase the work piece temperature, due to heat generated by frictional effects and plastic deformation. The induced softening allows the processing material to flow around the pin, from the front to the rear, resulting in a solid state weld. Temperature increase and high strain rate deformation lead to the formation of micro-structurally different zones: the nugget or stir zone (NZ) in the centre of the weld, surrounded by the thermo-mechanical affected zone (TMAZ) and the heat affected zone (HAZ).

This paper deals with the simulation of crack propagation in friction stir welded butt joints, in order to assess the influence of process induced microstructural alterations [1] and residual stresses on the fatigue behaviour of the assembly. The employed approach is based on the coupled usage of Finite Element Method (FEM) and Dual Boundary Element Method (DBEM) [2-3], in order to take advantage of the main capabilities of the two methods [4-7]. In particular, using the *Contour Method* [8], linear elastic stress analyses have been performed by FEM to evaluate the process induced residual stresses [9]. Then, the computed residual stresses field has been superimposed, in a DBEM environment, to the stress field due to a remote fatigue traction load and the crack growth is simulated. A two-parameters crack growth law, based on the evaluation of two thresholds, K_{maxth} and ΔK_{th}, for the material under analysis, is used for the crack propagation rate assessment [10-11]. The Stress Intensity Factors are evaluated by the J-integral technique [12-13]. Computational results have been compared with experimental data, provided by constant amplitude crack propagation tests on welded samples, showing the subdivision of the overall fatigue life in two periods, the crack initiation and crack propagation respectively.

2 Materials and Process Details

AA2024-T3 aluminium rolled plates have been joined by FSW. Plate dimensions are: 100 mm length, 30 mm width, and 4 mm thickness. The Young modulus is equal to 73.3 GPa and the Poisson coefficient equal to 0.33.

FSW processes have been executed normally to the rolling direction using a MCX 600 ECO machining centre. An AISI1040 quenched steel (56 HRC) tool with a conical pin has been employed (20 mm shoulder diameter, pin height 3.80 mm, pin diameter 6.20 mm, cone angle 30°). The tilt angle and the pin penetration have been assumed equal to 2 degrees and 0.2 mm, respectively. The tool rotating speed ω is

equal to 1400 rpm and feed rate v equal to 70 mm/min. The welding setup and the used tool are depicted in Figure 1.

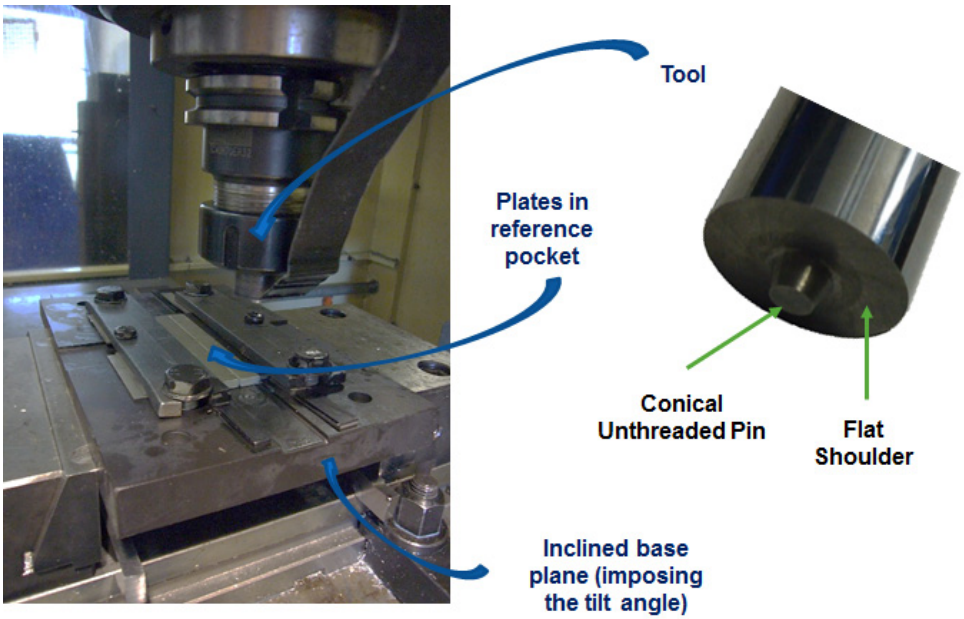

Figure 1: Welding setup and tool.

3 Crack Propagation experimental tests

The specimens were built with a central friction stir weld in order to assess the crack propagation along a line affected by the residual stresses caused by the FSW process (Figure 2).

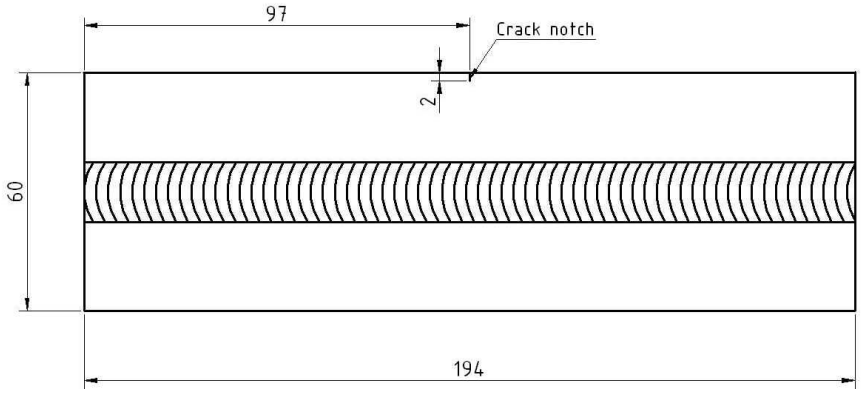

Figure 2: Specimen sizes (mm) and geometry.

In Figure 3 the fatigue tested specimen is shown: in order to localise the crack an initial edge notch, with a length equal to 2 mm, was cut by WEDM (Wire Electro Discharge Machining), in the middle of the specimen and two crack gages were applied on both sides of the notch in order to automatically monitor the advancing

crack. In particular, the crack growth was monitored using crack propagation patterns TK-09-CPA01-005/DP of MM Vishay.

The fatigue tests were performed on a universal testing machine INSTRON 8502. The tests were carried out using a load cell of 250 kN. A fatigue load P_{xmax} = 24 kN, (frequency equal to 10 Hz) was applied, with a load ratio R = 0.1.

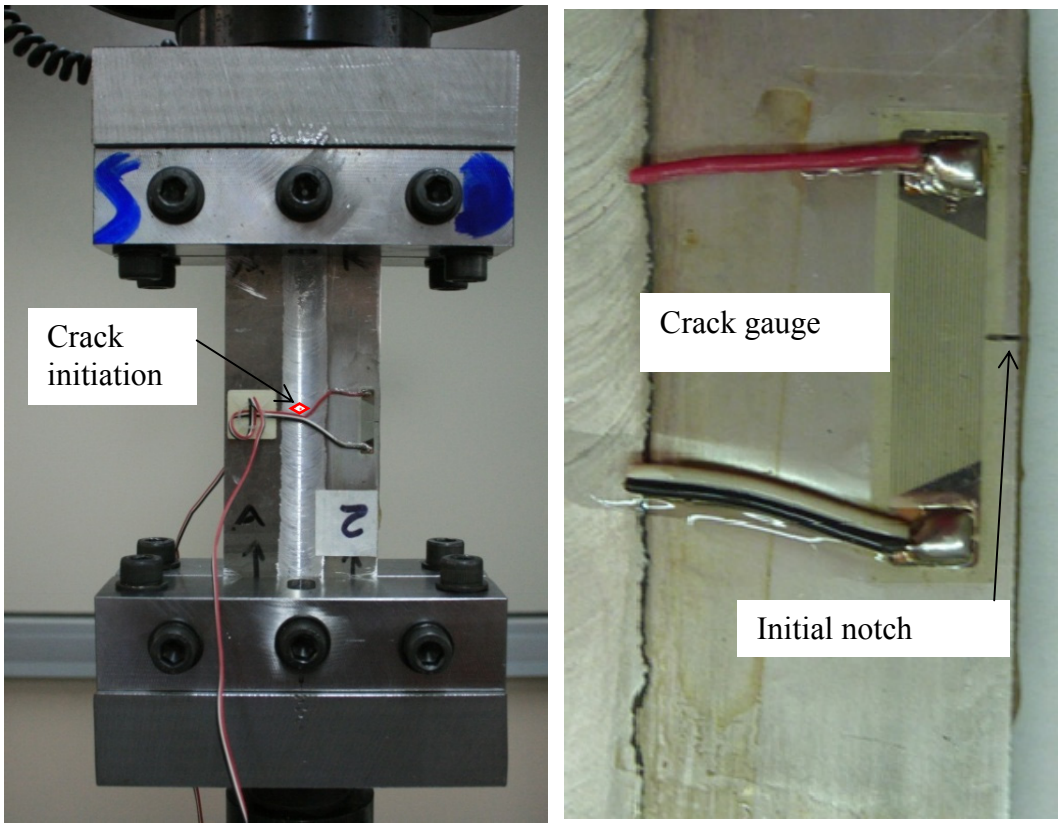

Figure 3: Experimental set-up with highlight of: specimen clamping in the fatigue machine and crack initiation area (left); notch and crack gauge close-up (right).

For the considered specimen, the crack initiated in a position different than expected (notch area), due to a superficial weld tunnel defect, which caused a strong localised material weakening, exactly in the middle of welding line as shown in Figures 3-4. Such an unexpected crack localisation did not represent a problem and was circumvented by changing the initiation point and initial crack geometry in the simulation (the residual stress scenario is known alongside the whole specimen section). The initial crack to be introduced in the numerical model was obtained by a post-mortem metallographic analysis of the specimen fracture surface (Figure 4): it is evident the separation between the crack propagation area and the area of static ductile failure, and the separation between the initial defect and crack propagation area. It is interesting to observe that a crack initiated in the middle of weld line, developed in a nearly symmetric shape indirectly validating the nearly symmetric

profile (Figure 5) of residual stress distribution in that area (the remote load induced stresses are clearly rigorously symmetric with respect the mid-plane of the weld).
The overall fatigue life of the analysed specimen was equal to 179000: the main part of such life, nearly 139000 cycles, was spent for crack initiation and the remaining 40000 cycles for crack propagation up to an unstable condition, as shown in the following.

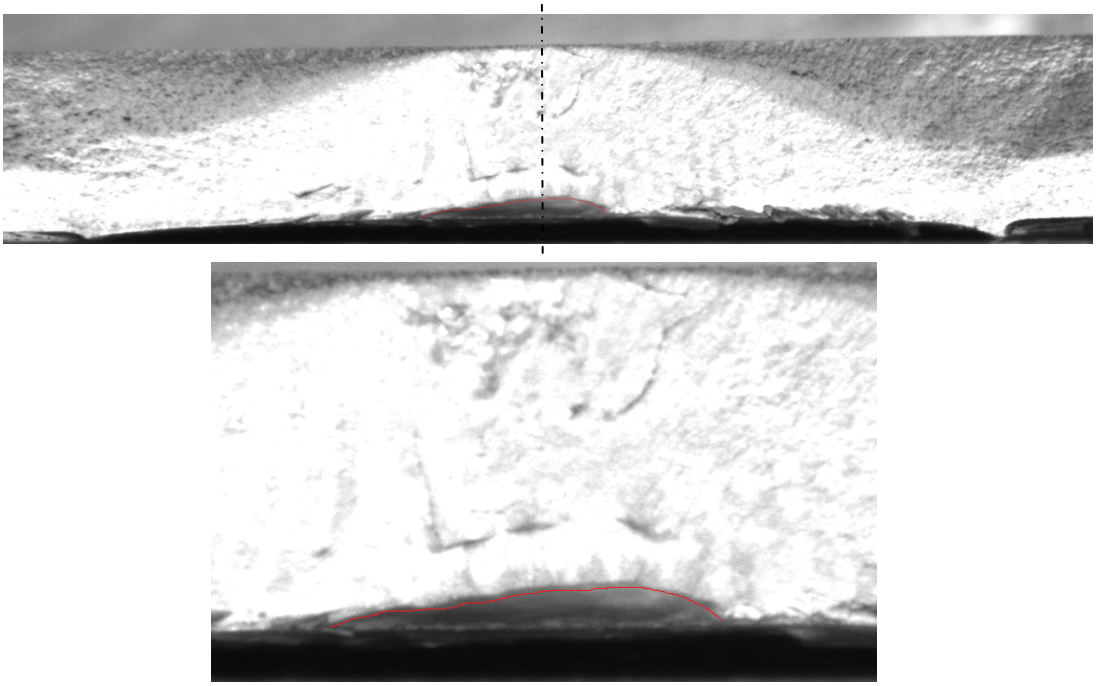

Figure 4: Crack propagation area with highlight of initial defect shape (red line) and weld mid-plane.

4 Crack Propagation modelling

4.1 Crack growth law

Residual stresses affect crack propagation since they change the effective value of the total Stress Intensity Factor (SIF) at the crack tip, with both the minimum (K_{min}) and the maximum (K_{max}) SIF values generally affected in the same way, so as to leave unchanged the parameter $\Delta K = K_{max}-K_{min}$. Consequently, the primary effect of residual stresses on crack growth rates are related to the K_{max} variations rather than to the ΔK variations. This is accounted for by the aforementioned two parameter approach: according to this theory, fatigue crack growth is driven by two driving forces, K_{max} and ΔK. Since it is assumed that, in presence of an overload, K_{max} also enters as the major driving force for fatigue crack growth, the corresponding residual stresses can affect crack growth rates even if they do not affect the parameter ΔK. In addition, the theory assumes that there are two fatigue thresholds, $K^*_{max,th}$ and ΔK^*_{th}

corresponding to the two driving forces: both the driving forces must be simultaneously larger than the relative thresholds for fatigue crack growth to occur. Since residual stress effects manifest primarily through a variation in K_{max} levels, an arrest in crack growth can occur if these stresses are compressive and sufficiently high to make the overall K_{max} falling below $K_{max,th}$. The crack growth law is assumed as follows [4-5]:

$$\frac{da}{dN} = A(\Delta K - \Delta K_{th}^{*})^{n}\left(K_{max} - K_{max,th}^{*}\right)^{m} \quad (1)$$

and is calibrated by best fitting the material parameters A, n, m based on literature data [14-15]. Used parameters are listed in Table 1. Such values are valid for every positive R-ratio.

ΔK^{*}_{th} (N/m$^{3/2}$)	$K^{*}_{max,th}$ (N/m$^{3/2}$)	A (m$^{1.5*(n+m)+1}$/N^{n+m})	n	m
1834121	3352014	6.745E-23	1.65	0.56

Table 1: Crack propagation law parameters

The friction stir welding effects are reproduced by taking into account the residual stress influence on the driving parameters ΔK and K_{max}. The residual stress effects are evaluated by considering the crack growth law represented by Equation (1), in which the SIF is defined as the sum of the nominal SIF, corresponding to the remote load, and of the SIF corresponding to the residual stresses acting on the crack faces and induced by the friction stir welding process.

The Bueckner approach [16] is adopted as derived from an application of the superposition principle. It states that the residual stress effect on the SIFs can be modelled by a distribution of tractions applied on the crack faces. Such tractions are obtained from the residual stresses, imported by the FEM code, existing on the virtual surface traced by the advancing crack (Figure 5). Only residual stresses in the direction normal to the crack plane are considered but this approximation is acceptable being the other components negligible, as also confirmed by the experimental outcome of a pure mode I crack propagation (Figure 4).

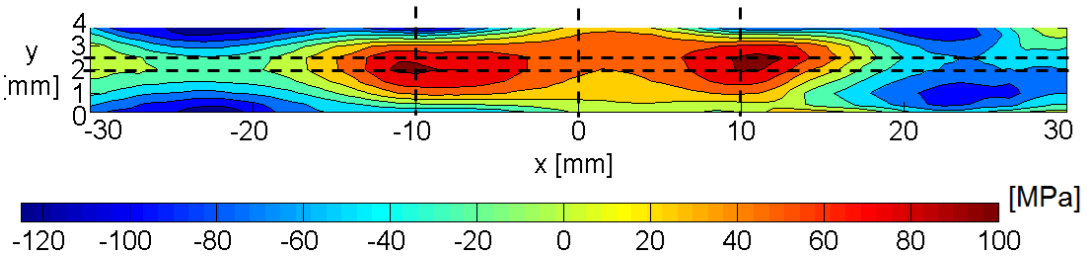

Figure 5: Longitudinal residual stresses (σ_{xx}) distribution from FEM analysis.

4.2 DBEM model and stress results

The following step is to realize a DBEM crack propagation analysis, with SIFs and crack growth rates calculated by J-integral technique and Vasudevan two parameter formula (Eq. 1) respectively. The mesh density is varying from the initial (Figures 6a-b) to the final (Figures 7a-b) crack configuration from nearly 1500 to 1800 *reduced quadratic elements* (the node at the element center is missing) respectively. The average crack advance along the crack front and at each step is equal to 0.7 mm. The initial crack has been modelled with a semielliptical crack front whose major and minor semi-axes are equal to 2.12 mm and 0.45 mm respectively.

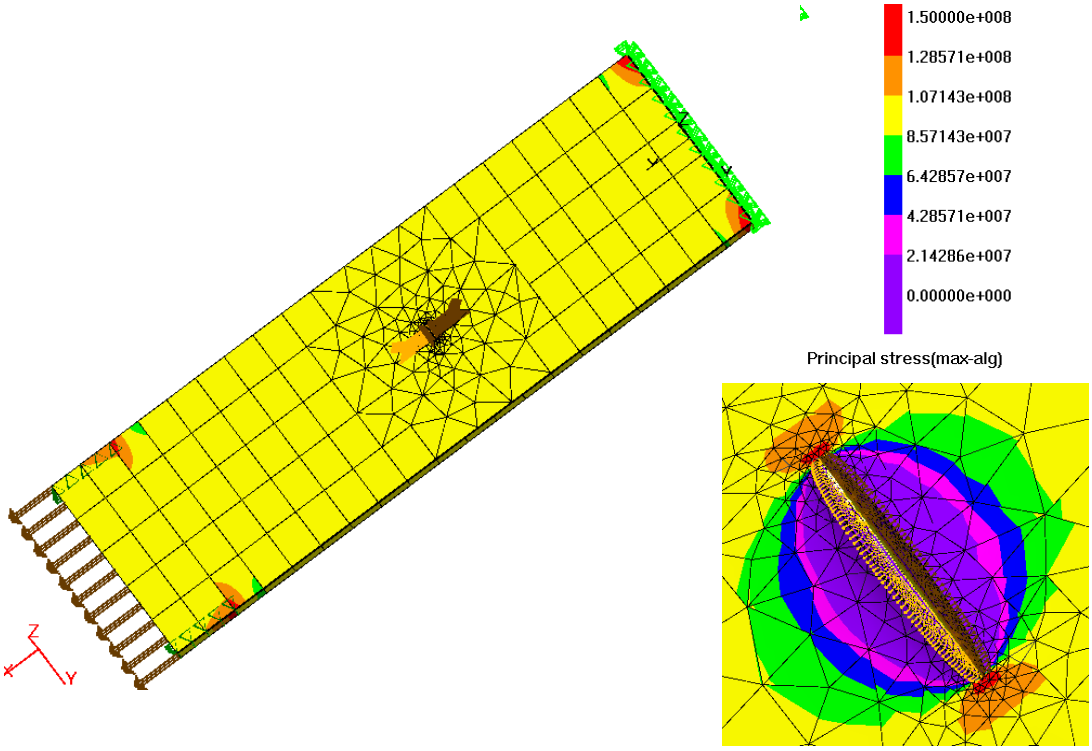

Figure 6a: DBEM initial cracked model with highlight of maximum principal stresses (MPa) and residual stresses on the crack faces.

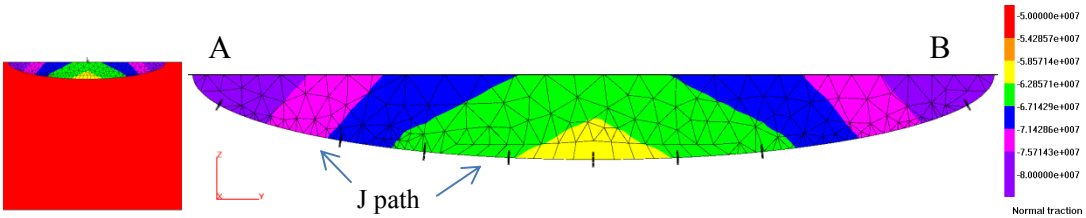

Figure 6b: DBEM initial cracked model with highlight of normal residual stresses (σ_{xx}) on the crack faces (MPa) and J-path along the crack front.

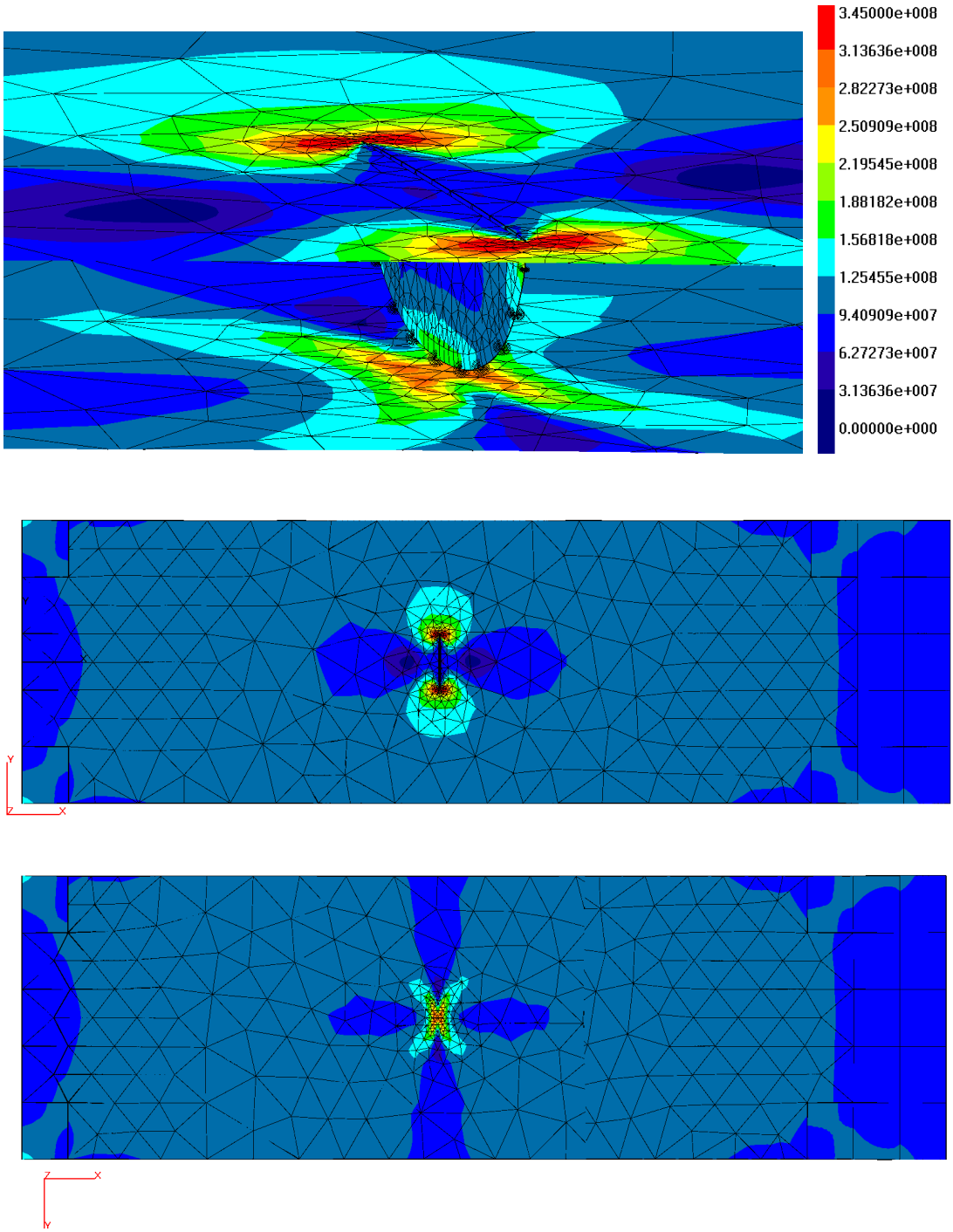

Figure 7a: DBEM final cracked model with highlight of Von Mises stresses (MPa) on both sides of specimen.

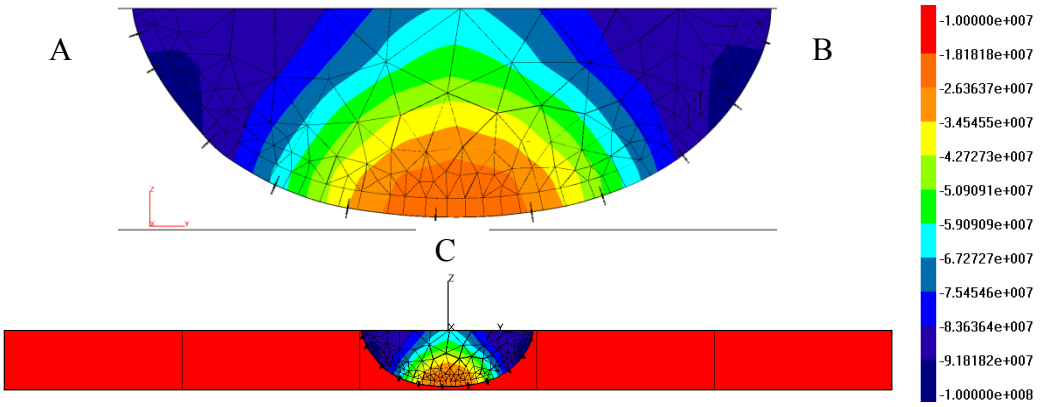

Figure 7b: DBEM final crack configuration with highlight of normal residual stresses (MPa) applied on crack faces and sizing point on crack front (A, B, C).

5 Crack Propagation results

After five crack growth steps the crack breaks through the thickness (Figures 7a-b) and the simulation stops: at this point the specimen will shortly fail (Figure 8) so there in no interest in continuing the simulation. This final crack front is still nearly semielliptical with major and minor semi-axes equal to 5.80 mm and 3.80 mm respectively. In Figure 9 SIFs along the crack front are displayed for each crack advance: it is possible to highlight the effect of the "opening" residual stresses which, in combination with the remote load, will speed up the crack propagation.

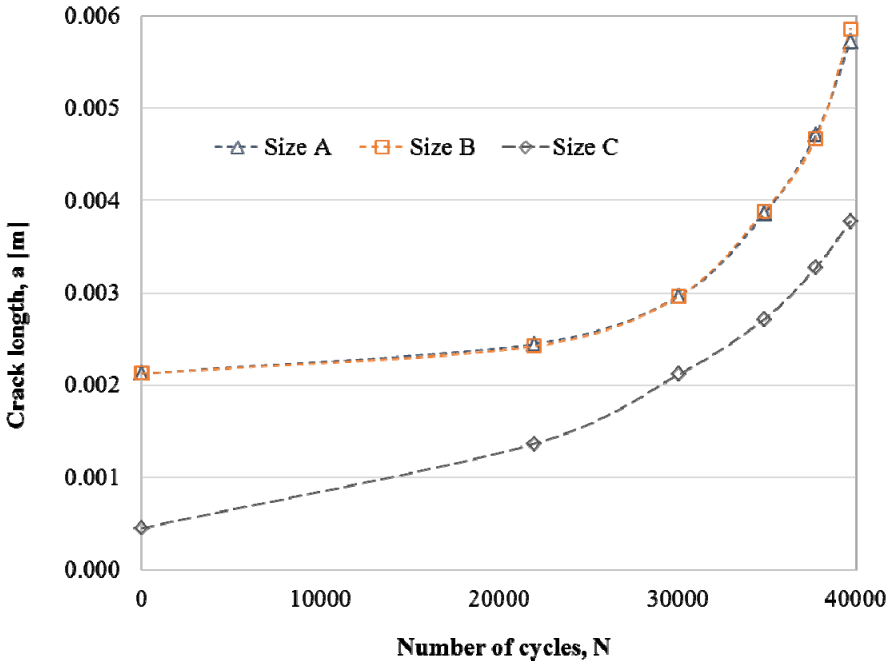

Figure 8: Crack sizes vs. number of cycles

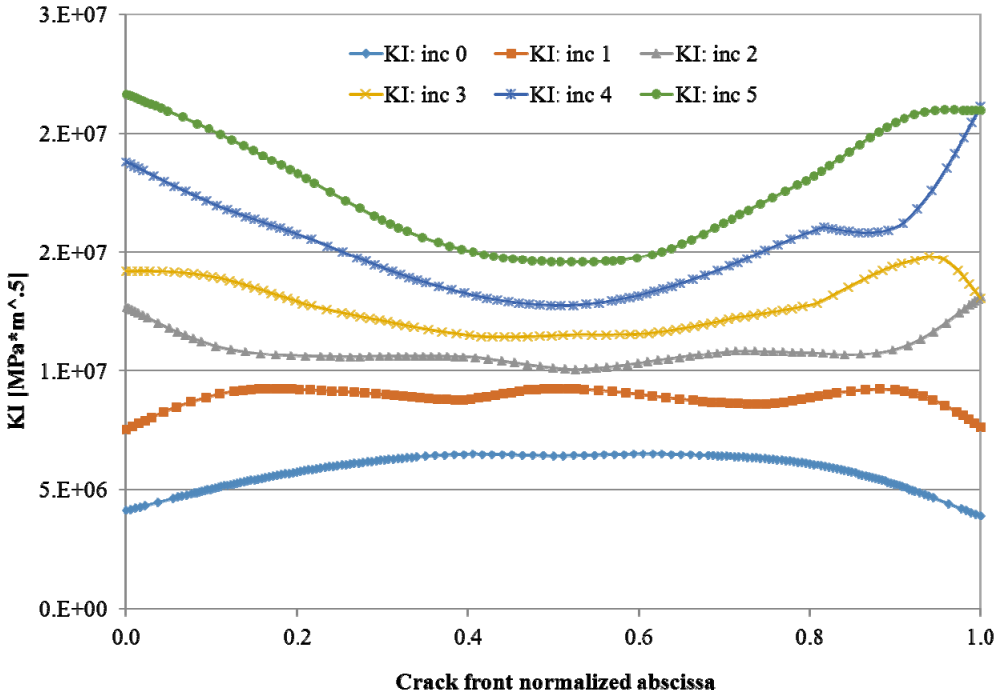

Figure 9: SIFs along the crack front for each step of crack propagation.

6 Conclusions

The following conclusions can be highlighted:

- the implemented FEM-DBEM approach can be considered as a powerful tool to predict the crack growth in presence of residual stresses induced by manufacturing processes;
- if the initial crack start from of the weld line the process induced opening stresses play an accelerating effect on the crack propagation;
- the crack propagation provided by the experimental test, characterized by pure mode I evolution and nearly symmetric shape (with respect to the weld line mid plane) qualitatively confirmed the residual stress numerical scenario;
- from a *post mortem* metallographic analysis the initial defect was clearly pointed out, allowing the definition of a realistic initial crack scenario for the numerical simulation; consequently a realistic assessment was provided for the crack propagation fraction of the overall fatigue life.

References

[1] P. Carlone, G.S. Palazzo (2013) Influence of Process Parameters on Microstructure and Mechanical Properties in AA2024-T3 Friction Stir Welding, Metallography, Microstructure, and Analysis 2:213-222.

[2] Y. Mi, MH. Aliabadi, “Dual boundary element method for three dimensional fracture mechanics analysis”, Engng Anal Boundary Elem, 10, 161–171, 1992.
[3] R. Citarella, G. Cricrì, E. Armentani (2013) Multiple crack propagation with Dual Boundary Element Method in stiffened and reinforced full scale aeronautic panels, Key Engineering Materials 560:129-155.
[4] R. Citarella, M. Lepore, J. Fellinger, V. Bykov, F. Schauer, Coupled FEM-DBEM method to assess crack growth in magnet system of Wendelstein 7-X, Frattura ed Integrità Strutturale, 26 (2013) 92-103.
[5] R. Citarella, G. Cricrì, M. Lepore, M. Perrella (2014) Thermo-Mechanical Crack Propagation in Aircraft Engine Vane by Coupled FEM-DBEM Approach, Advances in Engineering Software 67:57-69.
[6] R. Citarella, G. Cricrì, M. Lepore, M. Perrella, Assessment of Crack Growth from a Cold Worked Hole by Coupled FEM-DBEM Approach (2014) Key Engineering Materials 577-578:669-672.
[7] R. Citarella, G. Cricrì, Three-Dimensional BEM and FEM Submodelling in a Cracked FML Full Scale Aeronautic Panel, Appl Compos Mater (2014), doi: 10.1007/s10443-014-9384-5.
[8] M.B. Prime, “Cross-sectional mapping of residual stresses by measuring the surface contour after a cut”, J. Eng. Mater.-T, 123, 162-168, 2001.
[9] P. Carlone, G.S. Palazzo, “Longitudinal Residual Stress Analysis in AA2024-T3 Friction Stir Welding”, The Open Mechanical Engineering Journal 7, 18-26, 2013.
[10] R. Citarella, G. Cricrì, “A two-parameter model for crack growth simulation by combined FEM-DBEM approach”, Adv Eng. Softw., 40, 363-377, 2009.
[11] K. Sadananda, A.K. Vasudevan, “Short crack growth and internal stresses”, Int. J. Fatigue, 19, 99-108, 1997.
[12] RH. Rigby, MH. Aliabadi, “Mixed-mode J-integral method for analysis of 3D fracture problems using BEM”, Engng Anal Boundary Elem, 11, 239–561, 1993.
[13] RH. Rigby, MH. Aliabadi, “Decomposition of the mixed-mode J-integral – revisited”, Int J Solids Struct, 35(17), 2073–99, 1998.
[14] P. Carlone, R. Citarella, M. Lepore and G.S. Palazzo, “Numerical Crack Growth Analysis in AA2024-T3 Friction Stir Welded Butt Joints”, Proceedings of The Eighth International Conference on Engineering Computational Technology, 4-7 September 2012, Dubrovnik–Croatia.
[15] P. Carlone, R. Citarella, M. Lepore, G.S. Palazzo, “A FEM-DBEM investigation of the influence of process parameters on crack growth in aluminum friction stir welded butt joints”, International Journal of Material Forming (2014), (DOI) 10.1007/s12289-014-1186-7.
[16] H.F. Bueckner, “The propagation of cracks and the energy of elastic deformations”, Transaction of the ASME, 80, 1225-1230, 1958).